Journal of Chromatography A 1675 (2022) 463189

Contents lists available at ScienceDirect

Journal of Chromatography A

journal homepage: www.elsevier.com/locate/chroma

Optimization of enantiomer separation in flow-modulated comprehensive two-dimensional gas chromatography by response surface methodology coupled to artificial neural networks: Wine analysis case study

Olga Vyviurska[a], Nemanja Koljančić[a], Adriano A. Gomes[a,b], Ivan Špánik[a,*]

[a] Faculty of Chemical and Food Technology, Institute of Analytical Chemistry, Slovak University of Technology in Bratislava, Bratislava 81237, Slovak Republic
[b] Institute of Chemistry, Federal University of Rio Grande do Sul, Bento Gonçalves Avenue, 9500, Porto Alegre, RS 91501-970, Brazil

ARTICLE INFO

Article history:
Received 1 March 2022
Revised 29 May 2022
Accepted 31 May 2022
Available online 1 June 2022

Keywords:
Chiral separation
Flow-modulated comprehensive two-dimensional gas chromatography
Central composite analysis
Artificial neural networks
Tokaj wine region

ABSTRACT

In spite of extensive applications of flow modulated comprehensive two-dimensional gas chromatography (FM-GG × GC) in different research areas, its application in the field of chiral separation is very limited. From a practical point of view, the establishment of experimental parameters for enantiomer separations is possibly more demanding in this case. Since the carrier gas flows in both dimensions, it affects not only the separation parameters, but also the fill/flush volumes of the modulator and its working efficiency. In this context, a multivariate design of experiment was applied to find the optimum experimental parameters of a reversed fill/flush (RFF) modulator for enantiomer separation of organic compounds present in botrytized wine samples. The results were described both with response surface methodology and artificial neural networks (ANN). The enantiomeric composition of chiral compounds present in the botrytized wines was used to identify their geographical origin, by principal component analysis (PCA). In addition, the developed one-class partial least squares (OC-PLS) model enabled recognition of the wine samples from the Tokaj wine region with 93% effectiveness in the presence of other samples.

1. Introduction

Comprehensive two-dimensional gas chromatography (GC × GC) with thermal modulation generally dominates all omics studies, including food aroma characterization and analysis. On the other hand, continuous improvement of flow modulation technology in resolution, peak capacity and separation efficiency, supports the use of flow modulated comprehensive two-dimensional gas chromatography (FM-GC × GC) [1]. Currently, three flow modulators are commercially available for GC × GC analysis, namely a modulator based on Capillary Flow Technology (CFT), INSIGHT^{TM} modulator and FLUX^{TM} modulator. The Agilent CFT modulator [2] was developed based on a three-way solenoid valve and introduced in two arrangements: forward fill/flush (FFF) and reversed fill/flush (RFF). The RFF modulator was modified to overcome limitations of the FFF modulator, such as increased baseline and tailing in the second dimension (^{2}D) for high concentration components, as well as incomplete flushing of effluent from modulator capillary [3]. This was achieved through an additional bleeding capillary and down-up direction of the mobile phase during the flush phase [4]. Thus, ^{2}D peaks with a 135–147 ms baseline width was obtained for dodecane at 1–6 s modulation time [5]. Reversed fill/flush dynamics were also applied to the SepSolve INSIGHT^{TM} modulator, consisting of a single 7 port microchannel plate with a variable volume sample loop [6]. Dubois et al. [7] showed satisfactory results for baseline peak width (200–460 ms) and average tailing factor (1.16) for analysis of light volatile organic compounds. Recent developments in the fluidic modulator based on a solenoid valve [8] have led to introduction of the FLUX^{TM} modulator by LECO [9]. This modulator enables fast separation in the second dimension (a 700 ms modulation time) to achieve 240 ms ^{2}D peaks for major compounds in wines [10].

One of the limitations of exploiting the FM-GC × GC is the need for a more precise assignment of experimental conditions compared to thermal modulation. Overall, higher flow in the 2nd dimension (flush flow) over that in the 1st dimension (fill flow) is recommended for non-focusing modulators [11]. This enables compression of a peak slice and reduction of peak skewing in the second dimension. Several researchers have attempted to establish optimal experimental conditions with multivariate experimental design. For example, Valllejo et al. [12] combined a full-

* Corresponding author.
E-mail address: ivan.spanik@stuba.sk (I. Špánik).

https://doi.org/10.1016/j.chroma.2022.463189
0021-9673/

factorial experimental design with a screening step and central composite design at the optimization step for analysis of octyl- and nonylphenol isomers. In this case, peak symmetry, blob numbers and blob volumes were selected to define statistically significant experimental parameters (a 95% confidence interval) for the FFF modulator. Similar studies have been performed for analysis of hydrocarbons in lithic materials [13], volatile organic compounds in almonds [14] and terpenes in essential oils [15]. These also included a simplex approach for integrative optimization of some of the terpene responses. A simplex design was initially tested to achieve maximum distribution of C6–C12 aromatic hydrocarbons in the 2D separation space with the identical modulator [16]. Information entropy and synentropy percent were defined as the main parameters to determine flows in both dimensions and the temperature gradient. Synentropy percent was thus described by a quadratic model characterized with two maxima at 3D plot. Boegelsack et al. [17] compared Box-Behnken design and Doehlert design for optimization of FM-GC × GC for ignitable liquid residue analysis. Influence of inlet pressure, oven ramp and modulation period on average resolution in both dimensions and percent usage of the separation space were presented with response surface plots, indicating some differences in optimum between the designs. Furthermore, the authors used a Box-Behnken design for estimation of restrictor parameters for a time-of-flight mass spectrometer (TOFMS) and a flame-ionization detector (FID).

The importance of the calculation of fill and flush distances for carrier gas during one modulation cycle has been highlighted by Lelevic et al. [18], who demonstrated that total modulation distances should be comparable to a length of the modulation channel in order to exclude peak tailing for the FFF modulator. A pneumatic model has recently been presented to predict hold-up times and to define parameters of a bleed capillary of the RFF modulator [19]. In the case of a too restrictive bleed capillary, the authors showed the presence of a broad unmodulated peak in the second dimension as well as a retention time shift for the corresponding coeluted modulated peaks . On the other hand, loss of the first dimension (^{1}D) effluent could be observed through a bleed capillary for a prolonged modulation period with inappropriate instrumental parameters [5]. A retention model was suggested by Burel et al. [20] to predict retention times for FM-GC × GC. Calculations showed average errors of 0.44 and 2.2% for the ^{1}D time and ^{2}D time, respectively.

At the same time, a limited number of papers have been published on chiral analysis, which are mainly focused on the characterization of essential oils [21–23]. The advantages of enantioselective GC × GC research have been previously highlighted in wine analysis [24–27]. For example, enhanced separation efficiency of GC × GC improved precision in evaluation of enantiomeric distribution in complex samples, due to resolved coelutions with the second dimension. In our study, the multivariate optimization approach was tested to find optimal experimental parameters of the flow modulator, suitable for enantioselective evaluation of botrytized wines. The study also included artificial neural networks as a non-linear multivariate tool to describe a response surface for multivariate optimization.

2. Materials and methods

2.1. Chemicals, materials and samples

A mixture of alkanes (C7–C30) used for calculation of retention indexes was purchased from Supelco (Belleforte, PA). The standards of whiskey lactone, diethyl malate, 2,3–butanediol, α–terpineol, linalool, linalool oxide, terpinen–4–ol, ethyl lactate, γ–nonalactone, butanoic acid 2–methyl–ethyl ester, butanoic acid 2–hydroxy–3–methyl–ethyl ester, as well as pure enantiomers (S)–(−)–diethyl malate, (2R,3R)–(−)–2,3–butanediol, (R)–(−)–linalool, (S)–(+)–terpinen–4–ol, (S)–(−)–ethyl lactate, (R)–(+)–γ–nonalactone, (R)–(+)–limonene, (S)–(−)–limonene, (S)–(−)–β–citronellol, (R)–(+)–β–citronellol, (+)–rose oxide, (−)–rose oxide, and isomers of nerol, geraniol and *trans*–whiskey lactone were supplied by Sigma Aldrich (St. Louis, MO). R–(+)–α–terpineol and ethanol were provided by Fluka Chemicals (Fluka, Buchs, Switzerland) and Mikrochem (Pezinok, Slovakia), respectively. Organic solvents like hexane, dichloromethane and methanol were obtained from Merck (Darmstadt, Germany) and VWR Chemicals BDH (Gdansk, Poland).

Extraction was performed with SPE cartridges packed with 200 mg of LiChrolut EN resins in 3 mL polypropylene columns (Merck, Darmstadt, Germany).

Table 1 shows a list of analyzed wine samples as well as the codes used in the study. Botrytized wine samples (SK1-SK6, HU1-

Table 1
List of the analysed wine samples showing geographic origin, wine type and vintage.

No.	Manufacturer	Type	Vintage	Country	Code
1	Zlatý Strapec	3 putňa selection	2014	Slovakia	SK1
2	Zlatý Strapec	4 putňa selection	2008	Slovakia	SK2
3	Zlatý Strapec	5 putňa selection	2009	Slovakia	SK3
4	Zlatý Strapec	6 putňa selection	2009	Slovakia	SK4
5	Zlatý Strapec	6 putňa selection	2014	Slovakia	SK5
6	Tokaj & Co	6 putňa selection	2009	Slovakia	SK6
7	Sajgó Pincészet	Aszu 3 putňa	2008	Hungary	HU1
8	Sajgó Pincészet	Aszu 5 putňa	2006	Hungary	HU2
9	Sajgó Pincészet	Aszu 6 putňa	2013	Hungary	HU3
10	Simkó Pincészet	Aszu 3 putňa	2013	Hungary	HU4
11	Simkó Pincészet	Aszu 4 putňa	2013	Hungary	HU5
12	Simkó Pincészet	Aszu 5 putňa	2013	Hungary	HU6
13	Simkó Pincészet	Aszu 6 putňa	2014	Hungary	HU7
14	Simkó Pincészet	Aszu Eszencia	2008	Hungary	HU8
15	Way Fine & Provin	Muscat semi-sweet wine	2019	Hungary	HU9
16	Cotnar Hills Vineyard	Muscat wine	2015	Ukraine	UA1
17	Cotnar Hills Vineyard	Muscat wine	2017	Ukraine	UA2
18	Wenzel	Ruster Ausbruch - Am Fusse Des Berges	2006	Austria	AT1
19	Wenzel	Ruster Ausbruch - Am Fusse Des Berges	2007	Austria	AT2
20	Wenzel	Ruster Ausbruch - Saz	2005	Austria	AT3
21	Wenzel	Ruster Ausbruch - Saz	2007	Austria	AT4
22	Feiler-Artinger	Ruster Ausbruch	2017	Austria	AT5
23	Feiler-Artinger	Ruster Ausbruch - Essenz	2007	Austria	AT6
24	Feiler-Artinger	Ruster Ausbruch - Gelber Muscat	2015	Austria	AT7

HU7, UA1-UA2, AT1-AT5, AT7) and essences (HU8, AT6) included in the study originated from the Tokaj region in Slovakia and Hungary and the Austrian region of Burgenland. Two samples represented Muscat semi-sweet wines produced in the territory close to the Tokaj region. A 10-times diluted extract of UA2 sample (2017, Muscat wine, Cotnar Hills Vineyard, Ukraine) was used for optimization with central composite design.

2.2. Sample preparation

Solid-phase extraction was performed accordingly to the procedure described in [28]. The LiChrolut EN cartridges were conditioned with 4 mL of dichloromethane, 4 mL of methanol, and 4 mL of a water–ethanol mixture (12%, v/v). 50 mL of the wine sample was used at the extraction step and analytes were recovered by elution with 1.3 mL of dichloromethane.

2.3. GC × GC–MS/FID analysis

Flow modulated GC × GC–MS/FID analysis was performed on an Agilent 7890A Gas Chromatograph (Agilent Technologies, Santa Clara, CA, USA) equipped with a reverse fill/flush (RFF) modulator (Agilent Technologies, Santa Clara, CA, USA). Rt-ßDEXse chiral column (30 $m \times 0.25$ mm $\times 0.25$ µm, Restek, USA) was selected as the ^{1}D column and connected *via* the RFF modulator to an HP-INNOWAX ^{2}D column (5 $m \times 0.25$ mm $\times 0.15$ µm, Agilent Technologies, Santa Clara, CA, USA). The chiral column included a 2,3-di-O-ethyl-6-O–tert–butyl–dimethylsilyl-ß-cyclodextrin stationary phase. A bleeding capillary (5 $m \times 100$ µm ID) was attached to the modulator to support the carrier gas direction. Flush time of modulator was set to 0.11 s.

A volume of 1 µL of the extract was injected into a splitless injector heated at 220 °C. The initial temperature of the oven program was set to 40 °C with a hold time of 10 min. The temperature was then raised to a maximum of 220 °C with a 2 °C/min gradient and kept for 15 min. The measurements were carried out with a constant flow of helium (99.999%) over 115 min. The parameters that varied during optimization, like modulation time, and carrier gas flows in both dimensions (^{1}D and ^{2}D), are shown in Table 2. The wine samples were analyzed at 5 s modulation time, with a ^{1}D flow of 0.61 mL/min, ^{2}D flow of 28 mL/min.

After leaving the secondary column, the eluent was directed to a three-way splitter. A 0.5 $m \times 100$ µm ID restrictor and a 1.2 $m \times 250$ µm ID restrictor were connected to quadrupole MS and FID, respectively. The FID was operated at a temperature of 250 °C at a 100 Hz data acquisition rate. The temperatures of qMS and MS source were set to 180 °C and 300 °C. The mass spectrometer was operated at an acquisition rate of 12.75 spectra/s in the 40–400m/z range.

Table 2
Experimental conditions of central composite design.

Run	Block	*MT*, (s)	1F, mL/min	2F, mL/min
1	1	3.50	0.60	20.00
2	1	3.50	0.80	26.00
3	1	4.50	0.60	26.00
4	1	4.50	0.80	20.00
5	1	4.00	0.70	23.00
6	2	3.50	0.60	26.00
7	2	3.50	0.80	20.00
8	2	4.50	0.60	20.00
9	2	4.50	0.80	26.00
10	2	4.00	0.70	23.00
11	3	3.00	0.70	23.00
12	3	5.00	0.70	23.00
13	3	4.00	0.50	23.00
14	3	4.00	0.90	23.00
15	3	4.00	0.70	18.00
16	3	4.00	0.70	28.00
17	3	4.00	0.70	23.00

MT – modulation period; 1F – carrier gas flow in 1st dimension; 2F - carrier gas flow in 2nd dimension.

The processing of the chromatograms was primary performed with GC Image software version v. 2.1. (Zoex Corporation, Houston, TX, USA), and MSD ChemStation software (version F.01.01.2317, Agilent Technologies, Santa Clara, CA, USA) with NIST17, FFNSC2, MPW2007 and W9N11 databases. Identification of the compounds and elution order were confirmed with injection of standard compounds and pure enantiomers.

Enantiomeric composition of the chiral compounds was calculated based on GC × GC-FID data using the following equation:

$$ER = \frac{A_i}{\sum A} \times 100\% \quad (1)$$

where A_i represents area of modulated peaks of the dominant enantiomer and ΣA is total area of all enantiomers of the same compound. RSD values of area of dominant enantiomer ranged from 0.12 to 8.81% for SPE extraction and from 0.24 to 14.47% for GC × GC-FID injection.

2.4. Statistical evaluations

The optimizations of ^{1}D flow, ^{2}D flow and modulation period were established using a central composite design method. The experimental conditions varied in the range from 3 to 5 s for modulation time, from 0.5 to 0.9 mL/min for ^{1}D flow, and from 18 to 28 mL/min for ^{2}D flow (Table 2). The peak tailing at 10% of peak height was evaluated with MSD Chemstation Data Analysis software (Version F.01.01.2317, Agilent Technologies, Santa Clara, CA, USA). Average ^{2}D peak tailing of the modulated peaks related to the target compounds was used for model estimation. The second parameter applied for the multivariate optimization was a sum of ^{2}D peak areas of the target compound.

The obtained data were processed with Design of Experiment (DoE) module of the statistical software Statistica® (version 10.0). Pareto charts were used for evaluation of statistically significant effects ($p = 0.05$). The responses were first assessed with a second order polynomial function:

$$y = \beta_0 + \sum_{i=1}^{k} \beta_i x_i + \sum_{i=1}^{k} \beta_{ii} x_i^2 + \sum_{1 \le i \le j}^{k} \beta_{ij} x_i x_j + \varepsilon \quad (2)$$

where β_0 is an overall mean effect; β_i, β_{ii} and β_{ij} represent the coefficients of the first order, quadratic and interaction terms, respectively and ε is a random error component.

Artificial neural networks were applied to describe a relation between experimental parameters and responses (R1-R14). The calculations were performed with MatLab 2019a interface for multiple surface response optimization by artificial neural networks.

In order to carry out a preliminary evaluation of the data according to geographical origins, exploratory analysis was performed by principal component analysis with previously normalized data. One Class – Partial Least Square (OC-PLS) was used for rigorous one class classification, where Tokaj samples (both Slovak and Hungarian) were considered as a target class. The sample set was divided into target samples and the unknown samples using the Kernnard-Stone approach [29]. All calculations were carried out in MatLab 2019a environmental using PCA toolbox, OCPLS toolbox [30] and VStoolbox.

3. Results and discussion

3.1. Optimization

A central composite design was applied for optimization of experimental conditions for FM-GC × GC. The design included three independent factors (modulation time, ^{1}D and ^{2}D flows of the carrier gas) at five factor levels. These parameters affected the filling and flushing volumes of the RFF modulator, loss of eluent through the bleeding capillary as well as separation efficiency of GC × GC system, giving the peak area and ^{2}D peak tailing selected for model evaluation. Compounds with standard deviation of responses less than 10% at the central points were selected for data processing. The target group mainly included ethyl esters such as ethyl acetate, ethyl 2-methylpropanoate, ethyl lactate, and diethyl butanedioate as well as 2-phenylethanol, 1,2-propanediol and hexanoic acid. The objectives of the optimization procedure were (i) to maximize the area of peaks for trace analysis and (ii) minimize ^{2}D peak tailing for better peak separation.

In attempt to describe the results, response surface methodology based on a second order polynomial function was first used for model evaluations. Pareto charts with statistically significant effects defined with the ANOVA test ($p < 0.05$) were used to highlight significantly influential independent variances and their interactions. According to Fig. 1, area responses mainly depended on linear and quadratic terms of experimental parameters. A second order polynomial equation described area responses with the adjusted coefficients of determination for the model (R^2_{adj}) varied in the range of 0.761 to 0.972. Table 3 summarizes statistical evaluation of the proposed model and the obtained regression coefficients. A step-wise regression, namely backward regression, was applied to improve fitting for some compounds such as 1,2-propanediol, diethyl butanedioate and hexanoic acid. The selected models were successfully tested for significance of regression at $p < 0.05$. However, a lack of acceptable fit for ethyl acetate, ethyl 2-methylpropanoate and ethyl lactate was observed in the ANOVA test, suggesting that the selected model was too simple. More difficult was fitting of ^{2}D peak tailings with the multiple regression approach. Thus, all attempts to establish a statistically significant model with regression analysis were ineffective.

An artificial neural networks (ANN) approach was also tested as a tool for non-linear multivariate modeling. This is an information-processing chemometric technique that simulates the properties of the human mind [31]. In our case, responses including peak area and ^{2}D peak tailing of the selected compounds, were used for ANN architecture. As can be seen in Table 4, the ANN model provided the coefficient of determination (R^2) in the range of 0.76 to 0.99. A significant lack of fit test was only observed for two responses (no.2 and no.4) related to peak areas of ethyl 2-methylpropanoate and ethyl lactate, respectively. In order to find optimal conditions, individual desirability functions [32] for each response were computed using the ANN fitted models. Subsequently, all individual desirability functions were combined into a global desirability that made it possible to identify the best joint responses. Fig. 2 shows the 3D profile of the desirability values as well as level curves of desirability functions. As a result, the optimum experimental conditions were set as 0.61 mL/min for ^{1}D flow, 28 mL/min for ^{2}D flow and 5 s for modulation time. These parameters were further applied in to the chiral analysis of the wine samples under study.

3.2. Wine analysis

The optimized FM-GC × GC method was used for chiral analysis of the botrytized wines for classification purposes. GC × GC–MS chromatograms of the AT6 sample (Ruster Ausbruch Essenz 2007)

Table 3
Parameters of the response surface model.

Compound	R^2	R^2_{adj}	Intercept	Lack of Fit	MT	MT2	1F	1F^2	2F	2F	MT*1F	MT*2F	1F*1F
Ethyl acetate	0.985	0.967	***3.90E+07***	***0.016***	***−8.28E+06***	3.41E+05	−1.42E+07	−8.17E+06	−4.95E+05	−1.26E+04	2.30E+06	8.41E+04	***8.09E+05***
Ethyl 2-methylpropanoate	0.898	0.768	***2.35E+06***	***0.010***	−2.62E+05	1.45E+04	−1.39E+06	3.77E+05	***−8.73E+04***	***1.56E+03***	1.26E+05	−9.11E+01	1.55E+04
1,2-Propanediol	0.806	0.761	5.71E+05	***0.430***	pooled	***−2.16E+03***	pooled	pooled	***−4.04E+04***	***8.30E+02***	pooled	pooled	pooled
Ethyl lactate	0.963	0.915	***2.09E+06***	0.003	−1.54E+05	1.25E+04	1.63E+06	−7.42E+04	***−1.51E+05***	***2.63E+03***	−2.43E+05	5.39E+03	−1.30E+04
Hexanoic acid	0.809	0.745	7.47E+05	***0.210***	***−2.23E+04***	pooled	***5.66E+04***	pooled	***−5.24E+04***	***1.06E+03***	pooled	**pooled**	**pooled**
Diethyl butanedioate	0.955	0.940	5.00E+07	***0.480***	***−2.66E+06***	pooled	pooled	***6.02E+06***	***−2.59E+06***	***4.70E+04***	pooled	pooled	pooled
2-Phenylethanol	0.988	0.972	1.40E+08	***0.407***	−1.81E+07	9.04E+05	2.67E+07	1.45E+07	***−6.64E+06***	***9.24E+04***	−5.68E+06	3.50E+05	−9.77E+04

* -backwards step-wise regression; bolded coefficients are statistically significant ($p < 0.05$); R^2 -- coefficient of determination; R^2_{adj} - adjusted coefficient of determination; *MT* – modulation period; 1F – carrier gas flow in 1st dimension; 2F - carrier gas flow in 2nd dimension.

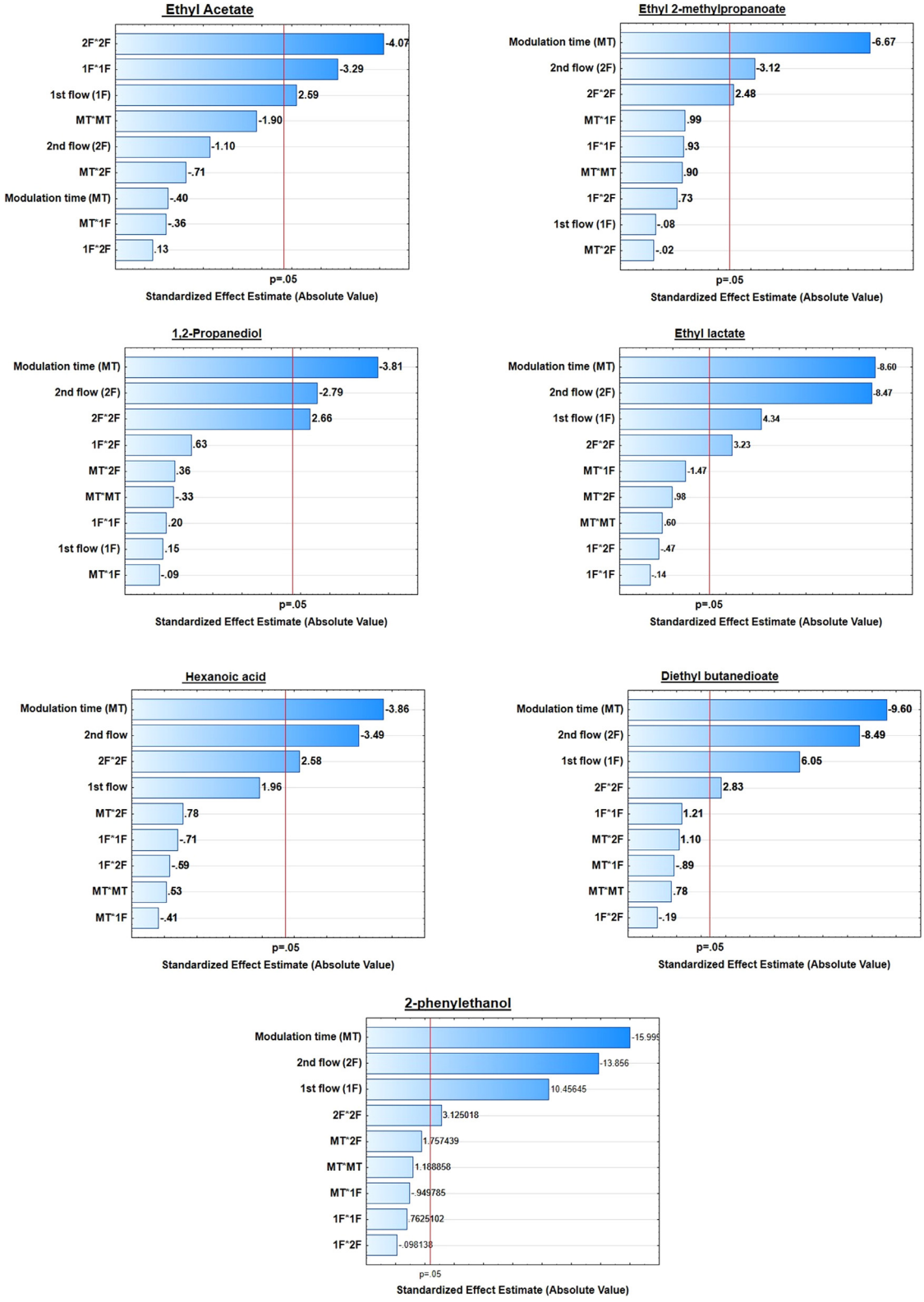

Fig. 1. Pareto charts for peak area responses of the selected volatile organic compounds. The reference lines indicate the $p = 0.05$ threshold for statistical significance effects.

can be seen in Fig. 3. The selected samples (Table 1) were produced in the Tokaj wine region (from both Slovakia and Hungary) and the Burgenland wine region (Austria). Production of these high-quality sweet wines requires a number of factors [33]; one of the most important is its specific climate conditions, favoring fermentation of grapes by *Botrytis cinerea*. Additional enzymatic processes that take place in rotting grapes affect color and aroma of the wine as well as the alcoholic and malolactic fermentation.

The selected chiral compounds belong to esters (ethyl lactate, diethyl malate, ethyl-2-methylbutyrate, ethyl 2–hydroxy-3-methyl butanoate), terpenoids (linalool oxide, nerol oxide, linalool, α-terpineol, terpinen-4-ol, β-citronellol, hotrienol) and lactones

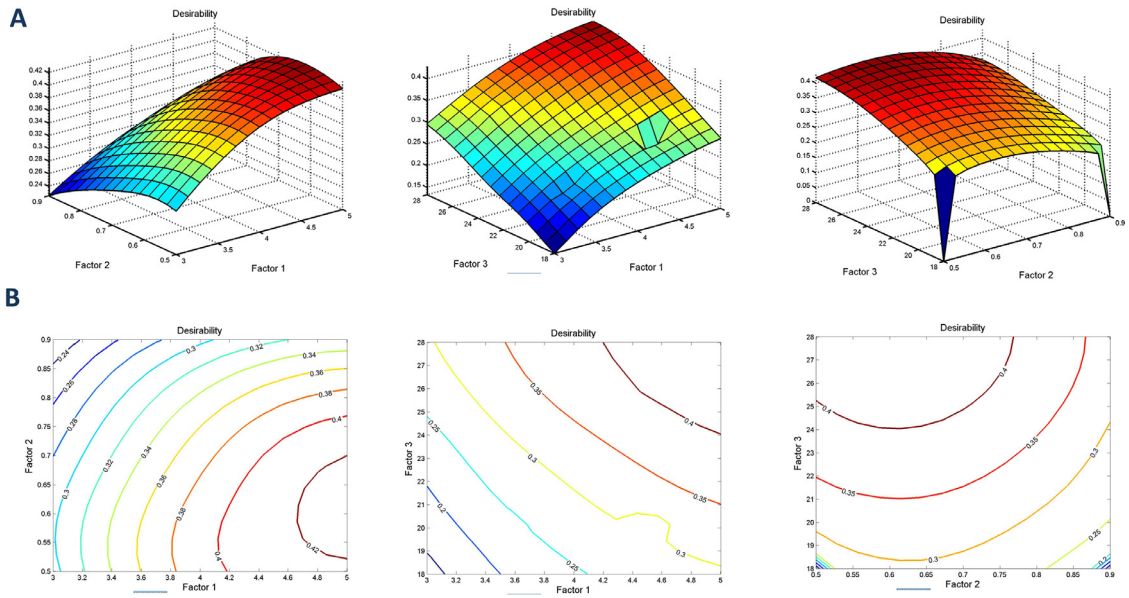

Fig. 2. A. 3D response surface plots (A) and contour plots (B) showing the effects of independent variables on desirability function. Factor 1 – Modulation time, s; Factor 2 – ^{1}D carrier gas flow, mL/min; Factor 3 – ^{2}D carrier gas flow, mL/min.

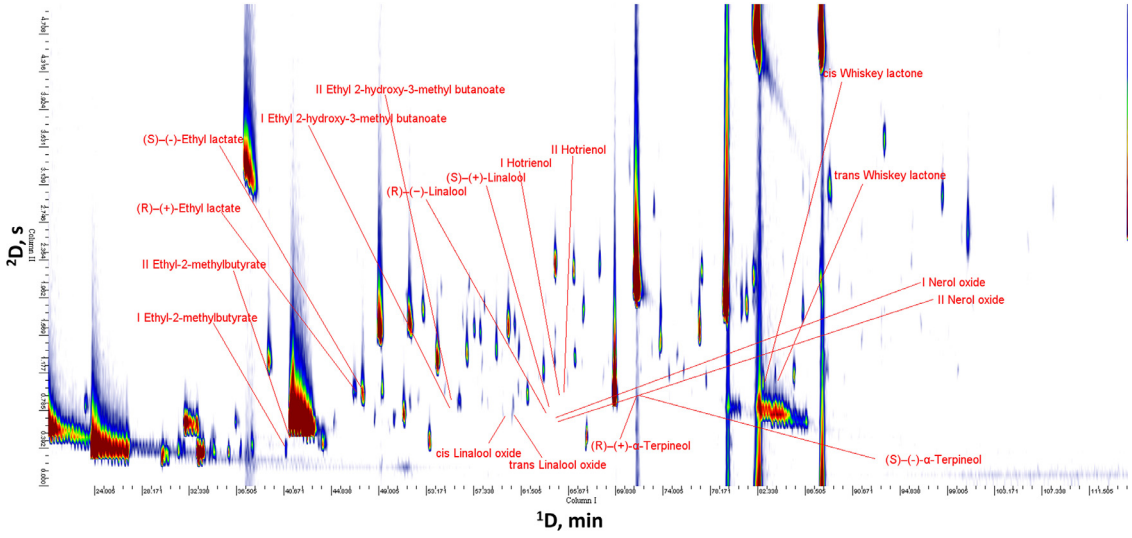

Fig. 3. GC × GC–MS chromatogram of Ruster Ausbruch Essense sample (2007). The target chiral compounds are shown on the chromatogram.

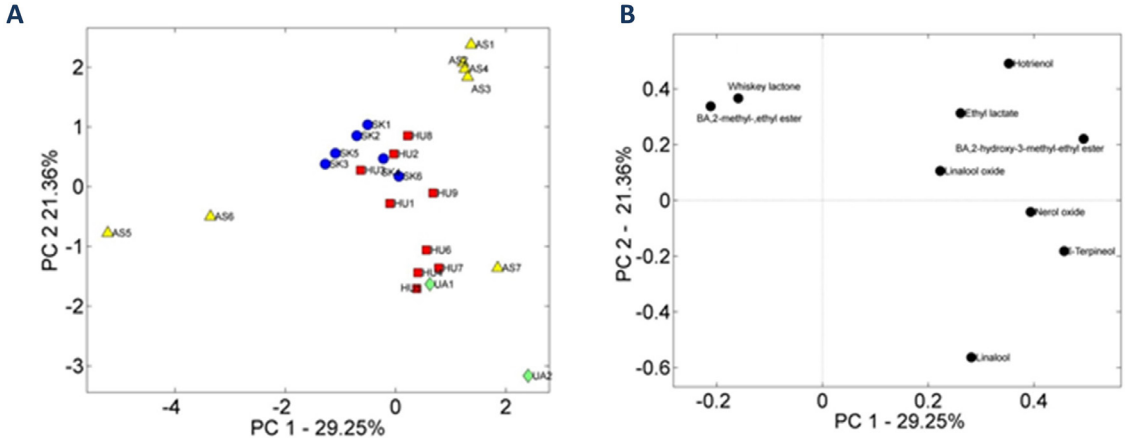

Fig. 4. Exploratory analysis by PCA using the results of chiral analysis: (A) bidimensional score plot and (B) plot of loadings. Classes: Austrian samples (▲), Slovak samples (●), Hungarian samples (■), Ukrainian samples (♦).

Table 4
ANN based optimization statistical summary.

Response	Architecture	R^2	[a]CV(%)	Lack of Fit
1	[3 11 1]	0.99	1.787	0.076
2	[3 5 1]	0.94	7.080	***0.030***
3	[3 5 1]	0.82	15.760	0.369
4	[3 7 1]	0.96	6.680	***0.005***
5	[3 5 1]	0.84	17.857	0.215
6	[3 7 1]	0.98	4.910	0.671
7	[3 7 1]	0.99	3.080	0.679
8	[3 5 1]	0.87	5.940	0.875
9	[3 13 1]	0.96	1.842	0.894
10	[3 4 1]	0.87	13.476	0.944
11	[3 8 1]	0.79	7.102	0.461
12	[3 6 1]	0.76	9.128	0.653
13	[3 13 1]	0.97	2.377	0.930
14	[3 13 1]	0.93	2.388	0.996

*coefficient of variance; R^2 -– coefficient of determination; bolded coefficients are statistically significant ($p < 0.05$).

(whiskey lactone and γ-nonalactone). In spite of the coelution of enantiomers of hotrienol and nerol oxide on the chiral column, these compounds were successfully separated in the second dimension with the polar HP-INNOWAX column.

A few compounds such as terpinen-4-ol, β-citronellol, γ-nonalactone and rose oxide were excluded from further data processing (Table 5), due to the presence of one enantiomer in the samples. For example, (*S*)-(+)-terpinen-4-ol and (*R*)-(+)- β–citronellol prevailed in Muscat semi-sweet wines (UA1 and UA2) produced in the territory located in the Ukraine, historically closed to Tokaj region. Rose oxide, (+)-enantiomeric form was identified in UA1 and AT7, representing the sample produced from the Muscat grape variety grown in the Burgenland wine region. This result could be related to the biotransformation of terpenes under influence of *Botrytis cinerea* [34]. On the contrary, γ-nonalactone compounds were not identified in UA samples; they appeared as (R)–(+)-form in the most of studied botrytized wine samples, expect for a racemic mixture in AT5 (Ruster Ausbruch, 2015). As reported previously in [35,36], an increased content of γ-nonalactone is typical of botrytized wines.

The results for the other chiral compounds are summarized in Table 5. A ratio between *trans* and *cis* stereoisomers for linalool oxide and whisky lactone was also included in the evaluation. The compounds were detected only in one enantiomeric form and a *trans/cis* ratio was tested as an additional tool for botrytized wine comparison. Contrary to our expectations, there was no significant difference between the samples with respect to geographical origin. A majority of the samples were described with similar dominance of one of stereoisomers for ethyl 2-methylbutyrate (67–100%), ethyl 2–hydroxy-3-methyl butanoate (60–100%) and hotrienol (67–95%). In contrast to SK and AT samples, linalool was present in most of the HU samples. A dominance of (*S*)-(+)-linalool (62–80%) was mainly observed in this case, except for UA2 and AS2, which were characterized with a racemate. Another racemic mixture was found for nerol oxide, which was not present in any of the SK samples.

Muscat semi-sweet wine (HU9) produced in the Hungarian part of the Tokaj wine region showed some differences in comparison to the local botrytized wines: a racemic mixture for ethyl 2–hydroxy-3-methylbutanoate and a dominance of (*R*)-(+)-ethyl lactate, both having previously been reported for varietal wines from Slovak part of Tokaj region [27]. These findings are inconsistent with those of the UA Muscat samples, where (*S*)-(-)-ethyl lactate prevailed.

Although the essence samples (HU8 and AT6) did not contain linalool, similar to the SK essences [27], other terpenoids such as α-terpineol and linalool oxides were present in both samples.

Table 5
Results of FM-GC × GC analysis of the selected samples.

Compound		RI	Retention time 1D, min	Retention time 2D, s	Samples SK1	SK2	SK3	SK4	SK5	SK6	HU1	HU2	HU3	HU4	HU5	HU6	HU7	HU8	HU9	AS1	AS2	AS3	AS4	AS5	AS6	AS7	UA1	UA2
Ethyl-2-methylbutyrate	I	893	40.84	0.47	96	96	81	77	84	91	87	82	76	83	72	86	76	73	70	67	31	87	75	88	89	100	74	100
	II	898	41.26	0.47	4	4	19	23	16	9	13	18	24	17	28	14	24	27	30	33	69	13	25	12	11	/	26	/
Ethyl lactate	(R)-(+)	969	46.84	0.94	32	31	32	29	29	33	49	49	34	19	18	16	33	29	92	38	34	68	67	51	44	13	31	43
	(S)-(-)	979	47.59	0.94	68	69	68	71	71	67	51	51	66	81	82	84	67	71	8	62	66	32	33	49	56	87	69	57
Linalool oxide	*cis*	1149	60.01	0.71	77	83	59	77	86	100	77	79	80	75	74	73	72	74	66	54	74	71	73	70	71	/	100	68
	trans	1167	61.26	0.71	23	17	41	23	14	/	23	21	20	25	26	27	28	26	34	46	26	29	27	30	29	/	/	32
Linalool	(R)-(−)	1200	63.59	0.71	/	/	/	/	/	20	40	22	11	38	35	30	38	/	33	27	50	/	/	/	/	/	/	51
	(S)-(+)	1205	63.92	0.79	/	/	/	/	/	80	60	78	89	62	65	70	62	/	67	73	51	/	/	/	/	/	/	49
Hotrienol	I	1218	64.76	1.02	18	14	8	16	6	9	10	12	8	7	5	10	11	28	9	12	13	29	30	29	33	/	/	12
	II	1224	65.17	0.94	82	86	92	84	94	91	90	88	92	93	95	90	89	72	91	88	87	71	70	71	67	/	/	88
Nerol oxide	I	1218	64.76	0.63	/	/	/	/	/	/	/	/	/	53	48	47	40	/	39	/	45	52	48	55	52	/	/	45
	II	1221	65.01	0.63	/	/	/	/	/	/	/	/	/	47	52	53	60	/	61	/	55	48	52	45	48	/	/	55
α-Terpineol	(S)-(-)	1330	72.17	0.94	63	59	46	62	44	83	76	78	69	66	65	79	76	68	68	79	77	48	48	51	49	/	/	80
	(R)-(+)	1325	71.84	0.94	37	41	54	38	56	17	24	22	31	34	35	21	24	32	32	21	23	52	52	49	51	/	/	20
Ethyl 2–hydroxy-3-methyl butanoate	I	1082	55.34	0.86	77	77	78	85	84	78	60	70	70	69	73	75	66	76	42	81	81	100	87	100	100	/	/	100
	II	1089	55.84	0.94	23	23	22	15	16	22	40	30	30	31	27	25	34	24	58	19	19	/	13	/	/	/	/	/
Whiskey lactone	*cis*	1503	82.92	1.1	41	42	50	40	54	63	69	80	78	39	40	41	36	39	62	/	/	51	54	37	39	39	38	/
	trans	1511	83.42	1.1	59	58	50	60	46	37	31	20	22	61	60	59	64	61	38	/	/	50	46	63	62	61	62	100

RI -retention index.

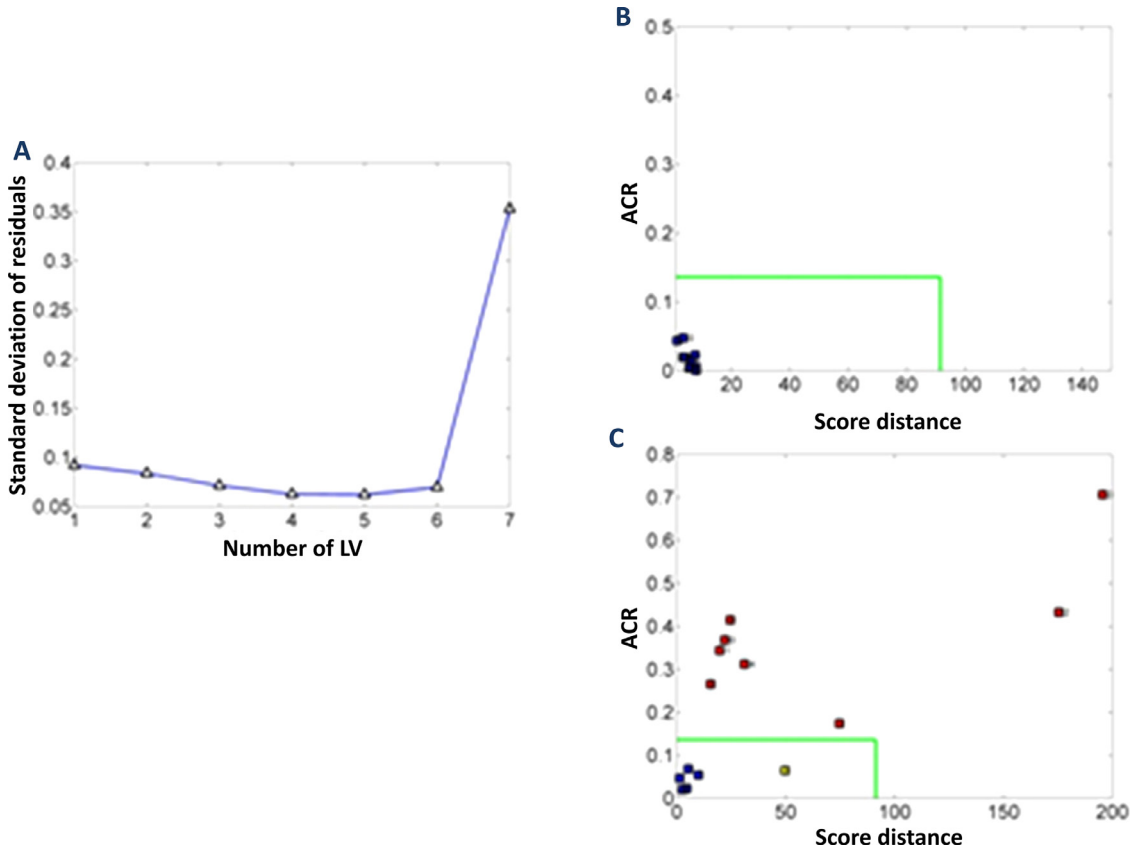

Fig. 5. OC-PLS model results: (A) optimal latent variable (LV) selection using acceptance area obtained in the training stage. OC-PLS plots of score distance *vs.* absolute centered residual (ACR) for training (B) and test (C) samples. The green lines are the limits of the acceptance area defined at 95% statistical confidence. The blue, red and yellow squares are the true positives, true negatives and false positives, respectively.

Our analysis showed some differences between the samples, *e.g.* absence of nerol oxides and dominance of (*S*)-(-)- α-terpineol in HU8. A similar situation with (*S*)-(-)-stereoisomer of α-terpineol was observed for a majority of the botrytized wines. A few samples (mainly AT botrytized wines) were characterized with a racemic mixture like the AT essence (AT6). An alteration in the technology for essence production, in contrast to the botrytized wines, should be noted. In this case, juice of botrytized berries obtained by gravity pressing during harvest season were used in the fermentation process [37]. According to our results, a variance between the selected essences and botrytized wines was mainly connected to the presence of linalool.

The data obtained were further processed with exploratory analysis by principal component analysis (PCA). As can be seen in Fig. 4A, a bi-dimensional score plot with around 50% of explained variance, showed a good segregation of the samples according to their geographical origin. SK and HU samples, in the figure, are characterized by an overlap, related to the geographical proximity of both wine regions. Historically, this was one wine region; it was divided in 1918 between Slovakia and Hungary. This group of vineyards is located in the central region of the plane defined by PC1 $\times$ PC2. Some of the other samples came from a more peripheral region. The loading graph shows linalool as the main parameter for distinction of the UA samples from other samples. The AT botrytized samples, on the other hand, were primary defined with hotrienol, whiskey lactone and ethyl 2-methylbutanoate (Fig. 4B). Overall, no significant dominance of any enantiomer of ethyl 2-hydroxy-3-methyl butanoate and ethyl-2-methylbutyrate was obtained. Further observations would suggest separation of the AS samples according to the producer. All botrytized wines (AT1-AT4) from Wenzel winery were located at the right top corner of the bi-dimensional score plot (Fig. 4A). The samples (AT5-AT7) produced by Feiler-Artinger winery required additional features to be compared.

At the same time, the data obtained were tested with the one-class partial least squares (OC-PLS) model. Six latent variables were sufficient to describe the rigorous OC-PLS model used for evaluation (Fig. 5A). At the training step, 10 Tokaj samples out of 15 were selected by the Kennard-Stone algorithm (Fig. 5B). The latent variables were defined by the acceptance area for the samples of the target class. Consequently, all samples were assigned to target class and the model reached 100% efficiency in the training stage.

Following this, Tokaj and non-Tokaj samples were evaluated as a test set. As can be seen in Fig. 5C, all five samples from the Tokaj region fell within the acceptance area, which confirmed effectiveness of the model effectivity. Further analysis showed that the model was also useful for recognition of non-Tokaj samples. Only one case was misclassified (highlighted as a yellow square in Fig. 5C). Overall, sensitivity, specificity and efficiency for the test step were estimated as 100%, 90% and 93%, respectively.

4. Conclusions

A combination of response surface methodology and artificial neural networks was applied for evaluation of optimal conditions of the RFF modulator for FM-GC $\times$ GC analysis of wine samples. The results of this study indicated a problem in describing the responses with least square methodology, especially for ^{2}D peak tailing. According to Pareto charts, the linear and quadratic terms of experimental parameters, such as modulation time and carrier gas flows in both dimensions, were statistically significant ($p<0.05$) for peak area response. Thus, ANN was selected as a nonparametric

tool for non-linear multivariate modeling and optimization. Chiral analysis of the botrytized wines was consequently performed under the optimized experimental conditions. Although a significant difference between the samples from different geographic origins was not established, a few tendencies in terpenes and terpenoids related to production technology were observed. In contrast to the botrytized wines, stereoisomers of linalool were not found in essences from either wine region. A smaller number of chiral terpenoids was observed for the samples from the Slovak part of the Tokaj region; this indicates variations in winemaking technologies between the wineries. Exploratory analysis by PCA enabled efficient identification of the Tokaj wine samples based on the results for enantiomeric distribution. The Ruster Ausbruch samples were separated accordingly to wine producer. In addition, the OC-PLS model was successful in recognizing Tokaj samples, with 100% efficiency at the training stage. 93% efficiency and 90% specificity of the model were achieved with the testing set in distinguishing of the target group in the presence of non-Tokaj samples.

Declaration of Competing Interest

The authors declare that they have no known competing financial interests or personal relationships that could have appeared to influence the work reported in this paper.

CRediT authorship contribution statement

Olga Vyviurska: Conceptualization, Methodology, Formal analysis, Writing – original draft, Visualization, Supervision. **Nemanja Koljančić:** Investigation, Formal analysis, Writing – original draft, Visualization. **Adriano A. Gomes:** Formal analysis, Visualization, Writing – review & editing. **Ivan Špánik:** Supervision, Writing – review & editing, Project administration, Funding acquisition.

Acknowledgements

The authors would like to acknowledge the financial support from Grant Agency of the Ministry of Education of Slovak Republic (contract VEGA 1/0521/19). A. A. G is grateful to CNPq for the scholarship (process 313381/2021–6)

Supplementary materials

Supplementary material associated with this article can be found, in the online version, at doi:10.1016/j.chroma.2022.463189.

References

[1] J. Krupčík, R. Gorovenko, I. Špánik, P. Sandra, D.W. Armstrong, Flow-modulated comprehensive two-dimensional gas chromatography with simultaneous flame ionization and quadrupole mass spectrometric detection, J. Chromatogr. A 1280 (2013) 104–111, doi:10.1016/j.chroma.2013.01.015.
[2] https://www.agilent.com/cs/library/brochures/5989-9889EN.pdf. (Accessed 07.02 2022).
[3] J.F. Griffith, W.L. Winniford, K. Sun, R. Edam, J.C. Luong, A reversed-flow differential flow modulator for comprehensive two-dimensional gas chromatography, J. Chromatogr. A 1226 (2012) 116–123, doi:10.1016/j.chroma.2011.11.036.
[4] https://www.agilent.com/cs/library/technicaloverviews/public/technicaloverview-gcxgc-reversed-flow-modulator-5994-0157en-agilent.pdf. (Accessed 07.02 2022).
[5] J. Krupčík, R. Gorovenko, I. Špánik, P. Sandra, M. Giardina, Comparison of the performance of forward fill/flush and reverse fill/flush flow modulation in comprehensive two-dimensional gas chromatography, J. Chromatogr. A 1466 (2016) 113–128, doi:10.1016/j.chroma.2016.08.032.
[6] https://www.srainstruments.com/wp-content/uploads/2020/04/INSIGHT-modulator.pdf. (Accessed 6.02 2022).
[7] L.M. Dubois, K.A. Perrault, P.H. Stefanuto, S. Koschinski, M. Edwards, L. McGregor, J.F. Focant, Thermal desorption comprehensive two-dimensional gas chromatography coupled to variable-energy electron ionization time-of-flight mass spectrometry for monitoring subtle changes in volatile organic compound profiles of human blood, J. Chromatogr. A 1501 (2017) 117–127, doi:10.1016/j.chroma.2017.04.026.
[8] J.V. Seeley, N.E. Schimmel, S.K. Seeley, The multi-mode modulator: a versatile fluidic device for two-dimensional gas chromatography, J. Chromatogr. A 1536 (2018) 6–15, doi:10.1016/j.chroma.2017.06.030.
[9] https://www.leco.com/product/flux. (Accessed 6.02 2022).
[10] P.E. Sudol, M. Galletta, P.Q. Tranchida, M. Zoccali, L. Mondello, R.E. Synovec, Untargeted profiling and differentiation of geographical variants of wine samples using headspace solid-phase microextraction flow-modulated comprehensive two-dimensional gas chromatography with the support of tile-based Fisher ratio analysis, J. Chromatogr. A 1662 (2022) 462735, doi:10.1016/j.chroma.2021.462735.
[11] P.M.A. Harvey, R.A. Shellie, Factors affecting peak shape in comprehensive two-dimensional gas chromatography with non-focusing modulation, J. Chromatogr. A 1218 (21) (2011) 3153–3158, doi:10.1016/j.chroma.2010.08.029.
[12] A. Vallejo, M. Olivares, L.A. Fernández, N. Etxebarria, S. Arrasate, E. Anakabe, A. Usobiaga, O. Zuloaga, Optimization of comprehensive two dimensional gas chromatography-flame ionization detection–quadrupole mass spectrometry for the separation of octyl- and nonylphenol isomers, J. Chromatogr. A 1218 (20) (2011) 3064–3069, doi:10.1016/j.chroma.2011.03.016.
[13] M. Olivares, M. Irazola, A. Vallejo, X. Murelaga, O. Zuloaga, N. Etxebarria, Comprehensive two-dimensional gas chromatography to characterize hydrocarbon mixtures in lithic materials, J. Chromatogr. A 1218 (12) (2011) 1656–1662, doi:10.1016/j.chroma.2010.11.034.
[14] P. Manzano, J.C. Diego, J.L. Bernal, M.J. Nozal, J. Bernal, Comprehensive two-dimensional gas chromatography coupled with static headspace sampling to analyze volatile compounds: application to almonds, J. Sep. Sci. 37 (6) (2014) 675–683, doi:10.1002/jssc.201301278.
[15] J. Omar, I. Alonso, M. Olivares, A. Vallejo, N. Etxebarria, Optimization of comprehensive two-dimensional gas-chromatography (GC×GC) mass spectrometry for the determination of essential oils, Talanta 88 (2012) 145–151, doi:10.1016/j.talanta.2011.10.023.
[16] P. Májek, J. Krupčík, R. Gorovenko, I. Špánik, P. Sandra, D.W. Armstrong, Computerized optimization of flows and temperature gradient in flow modulated comprehensive two-dimensional gas chromatography, J. Chromatogr. A 1349 (2014) 135–138, doi:10.1016/j.chroma.2014.05.015.
[17] N. Boegelsack, K. Hayes, C. Sandau, J.M. Withey, D.W. McMartin, G. O'Sullivan, Method development for optimizing analysis of ignitable liquid residues using flow-modulated comprehensive two-dimensional gas chromatography, J. Chromatogr. A 1656 (2021) 462495, doi:10.1016/j.chroma.2021.462495.
[18] A. Lelevic, V. Souchon, C. Geantet, C. Lorentz, M. Moreaud, Quantitative performance of forward fill/flush differential flow modulation for comprehensive two-dimensional gas chromatography, J. Chromatogr. A 1626 (2020) 461342, doi:10.1016/j.chroma.2020.461342.
[19] M. Giardina, J.D. McCurry, P. Cardinael, G. Semard-Jousset, C. Cordero, C. Bicchi, Development and validation of a pneumatic model for the reversed-flow differential flow modulator for comprehensive two-dimensional gas chromatography, J. Chromatogr. A 1577 (2018) 72–81, doi:10.1016/j.chroma.2018.09.022.
[20] A. Burel, M. Vaccaro, Y. Cartigny, S. Tisse, G. Coquerel, P. Cardinael, Retention modeling and retention time prediction in gas chromatography and flow-modulation comprehensive two-dimensional gas chromatography: the contribution of pressure on solute partition, J. Chromatogr. A 1485 (2017) 101–119, doi:10.1016/j.chroma.2017.01.011.
[21] J. Krupčík, R. Gorovenko, I. Špánik, P. Sandra, D.W. Armstrong, Enantioselective comprehensive two-dimensional gas chromatography. A route to elucidate the authenticity and origin of Rosa damascena Miller essential oils, J. Sep. Sci. 38 (19) (2015) 3397–3403, doi:10.1002/jssc.201500744.
[22] J. Krupčík, R. Gorovenko, I. Špánik, D.W. Armstrong, P. Sandra, Enantioselective comprehensive two-dimensional gas chromatography of lavender essential oil, J. Sep. Sci. 39 (24) (2016) 4765–4772, doi:10.1002/jssc.201600986.
[23] P.Q. Tranchida, G. Purcaro, A. Visco, L. Conte, P. Dugo, P. Dawes, L. Mondello, A flexible loop-type flow modulator for comprehensive two-dimensional gas chromatography, J. Chromatogr. A 1218 (21) (2011) 3140–3145, doi:10.1016/j.chroma.2010.11.082.
[24] A. Genovese, A. Gambuti, P. Piombino, L. Moio, Sensory properties and aroma compounds of sweet Fiano wine, Food Chem. 103 (4) (2007) 1228–1236, doi:10.1016/j.foodchem.2006.10.027.
[25] J. Sádecká, M. Jakubíková, P. Májek, Fluorescence spectroscopy for discrimination of botrytized wines, Food Control 88 (2018) 75–84, doi:10.1016/j.foodcont.2017.12.033.
[26] L. Khvalbota, A. Machyňáková, J. Čuchorová, K. Furdíková, I. Špánik, Enantiomer composition of chiral compounds present in traditional Slovak Tokaj wines, J. Food Compost. Anal. 96 (2021) 103719, doi:10.1016/j.jfca.2020.103719.
[27] O. Vyviurska, N. Koljančić, H.A. Thai, R. Gorovenko, I. Špánik, Classification of botrytized wines based on producing technology using flow-modulated comprehensive two-dimensional gas chromatography, Foods 10 (4) (2021), doi:10.3390/foods10040876.
[28] R. López, M. Aznar, J. Cacho, V. Ferreira, Determination of minor and trace volatile compounds in wine by solid-phase extraction and gas chromatography with mass spectrometric detection, J. Chromatogr. A 966 (1) (2002) 167–177, doi:10.1016/S0021-9673(02)00696-9.
[29] R.K.H. Galvão, M.C.U. Araujo, G.E. José, M.J.C. Pontes, E.C. Silva, T.C.B. Saldanha, A method for calibration and validation subset partitioning, Talanta 67 (4) (2005) 736–740, doi:10.1016/j.talanta.2005.03.025.
[30] L. Xu, M. Goodarzi, W. Shi, C.B. Cai, J.H. Jiang, A MATLAB toolbox for class modeling using one-class partial least squares (OCPLS) classifiers, Chemometr. Intell. Lab. Syst. 139 (2014) 58–63, doi:10.1016/j.chemolab.2014.09.005.

[31] L. Vera Candioti, M.M. De Zan, M.S. Cámara, H.C. Goicoechea, Experimental design and multiple response optimization. Using the desirability function in analytical methods development, Talanta 124 (2014) 123–138, doi:10.1016/j.talanta.2014.01.034.
[32] G. Derringer, R. Suich, Simultaneous optimization of several response variables, J. Qual. Technol. 12 (4) (1980) 214–219.
[33] I. Magyar, Botrytized wines, Adv. Food Nutr. Res. 63 (2011) 147–206, doi:10.1016/B978-0-12-384927-4.00006-3.
[34] G. Bock, I. Benda, P. Schreier, Biotransformation of Linalool by Botrytis cinerea, J. Food Sci. 51 (3) (1986) 659–662, doi:10.1111/j.1365-2621.1986.tb13904.x.
[35] E. Tosi, B. Fedrizzi, M. Azzolini, F. Finato, B. Simonato, G. Zapparoli, Effects of noble rot on must composition and aroma profile of Amarone wine produced by the traditional grape withering protocol, Food Chem. 130 (2) (2012) 370–375, doi:10.1016/j.foodchem.2011.07.053.
[36] T.E. Siebert, S.R. Barter, M.A. de Barros Lopes, M.J. Herderich, I.L. Francis, Investigation of 'stone fruit' aroma in Chardonnay, Viognier and botrytis Semillon wines, Food Chem. 256 (2018) 286–296, doi:10.1016/j.foodchem.2018.02.115.
[37] K. Furdíková, A. Machyňáková, T. Drtilová, I. Špánik, Comparison of different categories of Slovak Tokaj wines in terms of profiles of volatile organic compounds, Molecules 25 (3) (2020) 669, doi:10.3390/molecules25030669.